Fisher information in confined isotropic harmonic oscillator

Neetik Mukherjee and Amlan K. Roy*

Department of Chemical Sciences

Indian Institute of Science Education and Research (IISER) Kolkata,

Mohanpur-741246, Nadia, WB, India

arXiv:1904.03013v1 [quant-ph] 4 Apr 2019

Abstract

Fisher information (I) is investigated in a confined harmonic oscillator (CHO) enclosed in a spherical enclosure, in conjugate r and p spaces. A comparative study between CHO and a free quantum particle in spherical box (PISB), as well as CHO and respective free harmonic oscillator (FHO) is pursued with respect to energy spectrum and I. This reveals that, a CHO offers two exactly solvable limits, namely, a PISB and an FHO. Moreover, the dependence of I on quantum numbers n_r, l, m in FHO and CHO are analogous. The role of force constant is discussed. Further, a thorough systematic analysis of I with respect to variation of confinement radius r_c is presented, with particular attention on *non-zero*-(l, m) states. Considerable new important observations are recorded. The results are quite accurate and most of these are presented for the first time.

PACS: 03.65-w, 03.65Ca, 03.65Ta, 03.65.Ge, 03.67-a.

Keywords: Fisher Information, Particle in a spherical box, Confined isotropic harmonic oscillator.

*Corresponding author. Email: akroy@iiserkol.ac.in, akroy6k@gmail.com.

I. INTRODUCTION

Confined quantum systems have generated appreciable interest in the area of physics, chemistry, biology, [1–4], etc., since the first decade of this century. The simplest model system, namely, a particle in a D-dimensional spherical box, is used in textbooks to introduce fundamental ideas of quantum physics like the effect of boundary conditions, quantization of energy, linear superposition of wave etc. In such situations, the particle shows fascinating distinguishable changes in its observable physical, chemical properties [5, 6]. These models were designed to mimic real physical and chemical systems. In past two decades, behavior of confined systems with different potentials were explored quite vigorously. It has witnessed profound applications in a variety of research areas, like condensed matter, semiconductor physics, astrophysics, nano-science and technology, quantum dots, wires and wells [2, 4, 7], etc. Atomic, molecular confinement either in fullerene cage or inside the cavities of zeolite molecular sieves [2–4], were also pursued with great enthusiasm and promise.

A 1D confined harmonic oscillator (CHO) is considered as an intermediate model between particle in a box and free harmonic oscillator (FHO) [8, 9]. A variety of theoretical methods [10–14], such as semiclassical WKB, power-series solution, Padé approximation, perturbation theory, hypervirial theorem, Rayleigh-Ritz variation method, finding the zeros of confluent hypergeometric function numerically, imaginary-time evolution method etc., have been employed. Apart from the eigenspectrum, considerable efforts were directed towards Einstein co-efficients as well as information measures [9, 15–20] etc. Its 3D counterpart, i.e., the isotropic CHO centrally enclosed in a spherical box with impenetrable walls has been treated with equal intensity, using a number of theoretical methods, such as WKB, supersymmetric, properties of hypergeometric functions, quantization rule, generalized pseudospectral (GPS) method [13, 21–27]. It exhibits several unique degeneracy, splitting pattern as well as symmetry breaking, related to *simultaneous, incidental and inter-dimensional* degeneracy.

Over the years information theory has flourished as a pertinent field of study to revisit quantum mechanical problems. Apparently, this theory deals with single-particle probability density $\rho(\tau)$ of a system. In reality, information measures like Rènyi (R) and Shannon (S) entropy, Fisher information (I), Onicescu energy (E), quantify the spatial delocalization of $\rho(\tau)$, and hence can be explicitly employed in numerous interesting occurrences in quantum mechanics [2–4]. In a recent work present authors have thoroughly investigated all

these information theoretic measures (R, S, E, I and complexity) for confined hydrogen atom (CHA) [29–31]. Fundamentally, I quantifies expected error in a given measurement. By definition, it is a gradient functional of density. Because of its sensitivity toward local rearrangement of density, it is said to have property of locality [28]. Usually an increase in I suggests localization of $\rho(\tau)$. It is akin to the famous Weizsäcker kinetic energy functional ($T_\Omega[\rho]$) frequently employed in density functional theory [32]. It is also used in many other context such as to ascertain Pauli effects [33, 34], ionization potential, polarizability [35], entanglement [36], avoided crossing [37] in atomic physics, etc., to name a few. Exact analytical form of I in composite r, p-spaces for central potential have already been established in [38]. In [29, 30], authors have demonstrated the same relations for CHA. Further, I was explored for vibrational levels of various diatomic model potentials, such as Pöschl-Teller [39], pseudo-harmonic [40], Tietz-Wei [41], Frost-Musulin [42], Generalized Morse [43], exponential-cosine screened coulomb potential [44], etc.

The exact analytical form of I in conjugate r, p space for 3D FHO was reported in [38]. Some statistical complexities were investigated for Bohr-like orbits [45]. In 2016, S and R were computed for highly excited quantum states within Laguerre asymptotic approximation [46] and some linearized method [47]. However, an elaborate information theoretic study for 3D CHO is still lacking as of now. Hence, in this communication our primary objective is to perform a systematic analysis of I in a CHO, for any arbitrary state characterized by quantum numbers n_r, l, m, in both r and p spaces. Special attention has been paid to explore the effect of m on I, as well as *non-zero* l states. Illustrative calculations are executed with *exact* analytical wave functions in r-space whereas p-space wave functions are obtained from numerical Fourier transform of r-space counterpart. Specimen results are provided for $1s$-$1g$ as well as $2s$-$2m$ states. All the allowed m's corresponding to a given n_r and l have been taken into account, which provides the liberty to follow the definitive transformation in properties of states with m. Changes are also perceived with respect to oscillator frequency (ω). Since such works are very limited, most of present results are reported here for the first time. Section II gives a brief description about our theoretical method used; Sec. III offers a detailed discussion of results on I, while we conclude with a few comments in Sec. IV.

II. METHODOLOGY

The non-relativistic radial Schrödinger equation for an isotropic CHO, without any loss of generality, may be written as (atomic unit employed, unless otherwise mentioned),

$$\left[-\frac{1}{2}\,\frac{d^2}{dr^2}+\frac{\ell(\ell+1)}{2r^2}+v(r)+v_c(r)\right]\psi_{n_r,\ell}(r)=E_{n_r,\ell}\;\psi_{n_r,\ell}(r), \tag{1}$$

where $v(r)=\frac{1}{2}\omega^2 r^2$ and ω is the oscillator frequency. Our required confinement effect is induced by invoking the following form of potential: $v_c(r)=+\infty$ for $r>r_c$, and 0 for $r\leq r_c$, where r_c denotes radius of confinement.

Exact generalized radial wave function for a CHO is mathematically expressed as [25],

$$\psi_{n_r,l}(r)=N_{n_r,l}\;r^l\;{}_1F_1\left[\frac{1}{2}\left(l+\frac{3}{2}-\frac{\mathcal{E}_{n_r,l}}{\omega}\right),\left(l+\frac{3}{2}\right),\omega r^2\right]e^{-\frac{\omega}{2}r^2}. \tag{2}$$

Here $N_{n_r,l}$ signifies normalization constant, $\mathcal{E}_{n_r,l}$ corresponds to energy eigenvalue of a given state represented by n_r, l quantum numbers and ${}_1F_1\left[a,b,r\right]$ is a Kummer confluent hypergeometric function. Energies are calculated by assigning Dirichlet boundary condition, $\psi_{n_r,l}(0)=\psi_{n_r,l}(r_c)=0$ in Eq. (2). In this work, GPS method has been utilized to generate $\mathcal{E}_{n_r,l}$ of CHO. Over the years, this method has yielded very accurate results for a large number of model and real systems including atoms and molecules; this is well documented in the references [24, 27, 48–51] and therein.

The p-space wave function is obtained from Fourier transform of the r counterpart,

$$\psi_{n_r,l}(p)=\;\frac{1}{(2\pi)^{\frac{3}{2}}}\int_0^{r_c}\int_0^{\pi}\int_0^{2\pi}\psi_{n_r,l}(r)\;\Theta_{l,m}(\theta)\Phi_m(\phi)\;e^{ipr\cos\theta}r^2\sin\theta\;\mathrm{d}r\mathrm{d}\theta\mathrm{d}\phi. \tag{3}$$

Here $\psi(p)$ needs to be normalized. The normalized r- and p-space densities are represented as, $\rho(\mathbf{r})=|\psi_{n_r,l,m}(\mathbf{r})|^2$ and $\Pi(\mathbf{p})=|\psi_{n_r,l,m}(\mathbf{p})|^2$ respectively. Let $I_\mathbf{r}$, $I_\mathbf{p}$ denote *net* information measures in consequential r and p space of CHO. It is well established that, for a single particle in a central potential, these quantities can be written in terms of radial expectation values $\langle r^k\rangle$ and $\langle p^k\rangle(k=-2,2)$ [38], as below,

$$I_\mathbf{r}=\int_{\mathcal{R}^3}\left[\frac{|\nabla\rho(\mathbf{r})|^2}{\rho(\mathbf{r})}\right]\mathrm{d}\mathbf{r}=4\langle p^2\rangle-2(2l+1)|m|\langle r^{-2}\rangle \tag{4}$$

$$I_\mathbf{p}=\int_{\mathcal{R}^3}\left[\frac{|\nabla\Pi(\mathbf{p})|^2}{\Pi(\mathbf{p})}\right]\mathrm{d}\mathbf{p}=4\langle r^2\rangle-2(2l+1)|m|\langle p^{-2}\rangle. \tag{5}$$

The above equations can be further recast in following forms,

$$I_\mathbf{r}=8\mathcal{E}_{n_r,l}-8\langle v(r)\rangle-2(2l+1)|m|\langle r^{-2}\rangle \tag{6}$$

$$I_\mathbf{p}=8\mathcal{E}_{n_r,l}-8\langle v(p)\rangle-2(2l+1)|m|\langle p^{-2}\rangle. \tag{7}$$

where $v(p)$ is the p-space counterpart of $v(r)$.

In case of a CHO, I's in r and p space are expressed analytically as [52],

$$I_{\mathbf{r}}(\omega) = \frac{\omega}{\sqrt{2}} I_{\mathbf{r}}(\omega = 1), \qquad I_{\mathbf{p}}(\omega) = \frac{\sqrt{2}}{\omega} I_{\mathbf{p}}(\omega = 1). \tag{8}$$

Thus, an increase in ω leads to rise in $I_{\mathbf{r}}(\omega)$ and fall in $I_{\mathbf{p}}(\omega)$. However, it is obvious that I_t $(= I_{\mathbf{r}} I_{\mathbf{p}})$ remains invariant with ω. Throughout the article, for brevity, $I_{\mathbf{r}}(\omega = 1)$ and $I_{\mathbf{p}}(\omega = 1)$ will be symbolized as $I_{\mathbf{r}}$, $I_{\mathbf{p}}$ respectively.

When $m = 0$, $I_{\mathbf{r}}$ and $I_{\mathbf{p}}$ in Eqs. (4), (5) reduce to further simplified forms as below,

$$I_{\mathbf{r}} = 4\langle p^2 \rangle, \qquad I_{\mathbf{p}} = 4\langle r^2 \rangle. \tag{9}$$

It is seen that, at a fixed n_r, l, both $I_{\mathbf{r}}$ and $I_{\mathbf{p}}$ provide maximum values when $m = 0$, and both of them decrease with rise in m. Hence one obtains the following upper bound for I_t,

$$I_{\mathbf{r}} I_{\mathbf{p}} \ (= I_t) \leq 16 \langle r^2 \rangle \langle p^2 \rangle. \tag{10}$$

Further adjustment using Eqs. (6) and (7) leads to following uncertainty relations [38],

$$\frac{81}{\langle r^2 \rangle \langle p^2 \rangle} \leq I_{\mathbf{r}} I_{\mathbf{p}} \leq 16 \langle r^2 \rangle \langle p^2 \rangle. \tag{11}$$

Therefore, in a central potential, I-based uncertainty product is bounded by both upper as well as lower limits. They are state dependent, varying with n_r, l, m quantum numbers.

III. RESULT AND DISCUSSION

At the outset, it is instructive to note a few things for ease of discussion. Impact of quantum number m on $I_{\mathbf{r}}$ and $I_{\mathbf{p}}$ of CHO is one of the main objectives of our work; which is performed here for first time. Therefore, to ensure a desired accuracy of calculated quantities, a series of background tests were executed. The results in these tables are presented up to those points which sustained convergence. $I_{\mathbf{r}}$ values are obtained from Eqs. (4) and (6), whereas $I_{\mathbf{p}}$ from Eq. (5). In all occasions, it has been verified that, in both spaces, as $r_c \to \infty$, $I_{\mathbf{r}}$ and $I_{\mathbf{p}}$ converge to respective FHO limit. The *net* I in r and p spaces are divided into radial and angular part. But in both $I_{\mathbf{r}}$ and $I_{\mathbf{p}}$ expressions, angular contribution is normalized to unity. Hence, evaluation of all these targeted quantities using only radial part suffices our purpose. The radial wave function in r and p spaces depend only on n_r, l

TABLE I: $\mathcal{E}_{n_r,l}(n_r = 0)$ of lowest five circular states of CHO, PISB at five r_c. See text for details.

l	$r_c = 0.01$	$r_c = 0.05$	$r_c = 0.1^{\dagger}$	$r_c = 0.2$	$r_c = 0.5^{\dagger}$
			CHO		
0	49348.02202373	1973.92123372	493.48163345	123.37570844	19.77453418
1	100953.64280465	4038.14617967	1009.53830088	252.39159906	40.42827649
2	166087.30959293	6643.49293120	1660.87528919	415.22704789	66.48975653
3	244155.96823805	9753.60193720	2441.56211674	610.39965899	97.72324914
4	334771.55964446	13390.86304096	3347.71822121	836.93939916	133.97424683
			PISB		
0	49348.022005446	1973.92088021	493.48022005	123.37005501	19.73920880
1	100953.64278213	4038.14571128	1009.53642782	252.38410695	40.38145711
2	166087.30957134	6643.49238285	1660.87309571	415.21827392	66.43492382
3	244155.96821809	9753.60153136	2441.55968218	610.38992054	97.66238728
4	334771.55962552	13390.86238502	3347.71559625	836.92889906	133.90862385

†1st three l-energies are taken from [14]; the remaining ones are freshly generated in this work.

quantum numbers. Hence, in both space, radial wave function can be obtained by putting $m = 0$ in Eq. (3). Further, a change in m from *zero* to *non-zero* value will not influence the expression of radial wave function in p space. Confinement in isotropic harmonic oscillator is attained by squeezing the radial boundary from infinity to a finite region. To realize these, pilot calculations are done for $1s$-$1g$ and $2s$-$2m$ states, with r_c varying from 0.1 to 7 a.u. The former set is chosen as they represent nodeless ground states corresponding to various l, whereas, $2s$-$2m$ states are considered to perceive the effect of nodes on I at *non-zero* m. Also note that, we have followed the spectroscopic notation, i.e., the levels are denoted by $n_r + 1$ and l values (see, e.g., [49]). Therefore, $n_r = 0$ and $l = 4$ signifies $1g$ state. The radial quantum number n_r relates to n as $n = 2n_r + l$.

Exact analytical form of $I_{\mathbf{r}}$ and $I_{\mathbf{p}}$ in isotropic FHO was given in [38],

$$I_{\mathbf{r}}(\omega) = 4\omega \left(2n_r + l - |m| + \frac{3}{2}\right), \quad I_{\mathbf{p}}(\omega) = \frac{4}{\omega}\left(2n_r + l - |m| + \frac{3}{2}\right). \tag{12}$$

It suggests that, at a fixed m, both $I_{\mathbf{r}}(\omega), I_{\mathbf{p}}(\omega)$ increase as n_r and l approach higher values. Similarly, for a specific n_r and l, both $I_{\mathbf{r}}(\omega), I_{\mathbf{p}}(\omega)$ abate with growth in $|m|$. Influence of ω on $I_{\mathbf{r}}(\omega)$ and $I_{\mathbf{p}}(\omega)$ is quite straightforward. $I_{\mathbf{r}}(\omega)$ progresses and $I_{\mathbf{p}}(\omega)$ reduces with rise of ω. By putting $\omega = 1$ in Eq. (12) one easily gets the expressions for $I_{\mathbf{r}}$ and $I_{\mathbf{p}}$ in a FHO.

At first we illustrate the behavior of CHO at $r_c \to 0$. A careful study exposes that, at small r_c, CHO has an energy spectrum comparable to that of a particle in a spherical

TABLE II: $I_{\mathbf{r}}, I_{\mathbf{p}}$ of lowest five circular states of CHO and PISB at five r_c at fixed m (0).

System	l	$r_c = 0.01$	$r_c = 0.05$	$r_c = 0.1$	$r_c = 0.2$	$r_c = 0.5$
			$I_{\mathbf{r}}$			
	0	394784.17618984	15791.36986976	3947.84176	986.960440	157.913740
	1	807629.1424372	32305.16943736	8076.29142	2019.072855	323.051708232
CHO	2	1328698.47674344	53147.9434496	13286.984765	3321.7461915	531.4794285
	3	1953247.7459044	78028.8154976	19532.47745	4883.119364	781.2991270
	4	2678172.47715568	107126.90432768	26781.72476	6695.431192	1071.269013
	0	394784.17604357	15791.36704174	3947.84176043	986.96044010	157.91367041
	1	807629.14225706	32305.16569028	8076.29142257	2019.07285564	323.05165690
PISB	2	1328698.47657073	53147.93906282	13286.98476570	3321.74619142	531.47939062
	3	1953247.74574476	78028.81225090	19532.47745744	4883.11936436	781.29909829
	4	2678172.47700420	107126.89908016	26781.72477004	6695.43119251	1071.26899080
			$I_{\mathbf{p}}$			
	0	0.000113069096	0.00282672727	0.01130690073	0.045227067368	0.28253330127
	1	0.00014984256	0.00374606392	0.01498424952	0.05993660387	0.3745037429
CHO	2	0.00017547984	0.004386995939	0.0175479792	0.0701916254	0.4386237207
	3	0.000194769472	0.004875545605	0.0194769435	0.0779075530	0.4868660984
	4	0.000210002530	0.005250063214	0.0210002501	0.0840008284	0.5249614675
	0	0.000113069096	0.00282672741	0.01130690966	0.04522763864	0.28267274151
	1	0.0001498425609	0.00374606402	0.01498425609	0.05993702437	0.374n60640235
PISB	2	0.0001754798406	0.00438699601	0.01754798406	0.07019193624	0.43869960150
	3	0.0001947694723	0.00486923680	0.01947694723	0.07790778893	0.48692368082
	4	0.0002100025303	0.00525006325	0.02100025303	0.08400101214	0.52500632592

box (PISB). This trend generally holds good for all other states as well. A cross-section of eigenvalues ($1s$-$1g$) of lowest five circular states corresponding to l = 0-4, of CHO and PISB, presented in Table I, at five selected r_c, *viz.*, $0.01, 0.05, 0.1, 0.2, 0.5$, supports this fact. However this observation should not be misconstrued to conclude that at $r_c \to 0$, CHO leads to PISB. Because that can happen only when both systems have nearly equal kinetic energy as well as potential energy components. This is not directly discernible from this table. At this point, it is worthwhile mentioning that, like CHO, PISB is also exactly solvable; eigenfunctions are expressible directly in terms of first-order Bessel function, and given as,

$$J_l(Z) = (-1)^l Z^l \left(\frac{1}{Z}\frac{d}{dZ}\right)^l \left(\frac{\sin Z}{Z}\right), \tag{13}$$

where $Z = \sqrt{\mathcal{E}_{n_r,l}}\, r$. At the boundary when $r = r_c$, $Z = Z_{n_r,l}$ and $J_l(Z_{n_r,l}) = 0$. Moreover, at $r = r_c$, the energy of a (n_r, l) state is expressed as $\mathcal{E}_{n_r,l} = \frac{Z^2_{n_r,l}}{r_c^2}$ [53]. This $J_l(Z_{n_r,l}) = 0$ is a transcendental equation and at a fixed n_r, l, this $Z_{n_r,l}$ is evaluated by the help of MATHEMATICA program package. Thus all the PISB energies in lower segment of this

TABLE III: $I_{\mathbf{r}}, I_{\mathbf{p}}$ of $1p, 1d, 1f$ states of CHO at six r_c, with varying m. Results in last column correspond to respective FHO values, computed from Eq. (12). See text for details.

$\|m\|$	$r_c = 0.1$	$r_c = 0.5$	$r_c = 1$	$r_c = 2$	$r_c = 7$	$r_c = \infty$
			$I_{\mathbf{r}}(1p)$			
0	8076.29142	323.051708232	80.76619765	20.39764116	10.0000000000	10
1	5736.542528	229.424233922	57.21792995	13.916600785	6.0000000000	6
			$I_{\mathbf{p}}(1p)$			
0	0.014984249523	0.374503742927	1.491857857098	5.577935621669	10.00000000	10
1	0.01003	0.2507	0.9980	3.975	6.0000	6
			$I_{\mathbf{r}}(1d)$			
0	13286.984765	531.4794285	132.8722779	33.374501702	14.0000000000	14
1	10419.849672	416.7666252	104.09083474	25.745587549	10.0000000000	10
2	7552.714578	302.0538220	75.3093915	18.11667339	6.0000000000	6
			$I_{\mathbf{p}}(1d)$			
0	0.017547979204	0.438623720749	1.749938940164	6.705825222118	14.000000000	14
1	0.0133333	0.33326	1.32905	5.0595	10.00000	10
2	0.0091187	0.2279	0.9081	3.4132	6.00000	6
			$I_{\mathbf{r}}(1f)$			
0	19532.47745	781.2991270	195.3266196	48.95155358	18.000000000	18
1	16156.649498	646.2448005	161.48315319	40.15669405	14.00000000	14
2	12780.8215	511.1904739	127.63968669	31.36183453	10.00000000	10
3	9404.993581	376.1361474	93.79622020	22.566975007	6.000000000	6
			$I_{\mathbf{p}}(1f)$			
0	0.019476943548	0.486866098432	1.944005783407	7.551236509511	18.0000000	18
1	0.0157907758	0.39471708	1.57572258	6.0995039	14.00000	14
2	0.012104608	0.30256807	1.20743938	4.6477714	10.00000	10
3	0.008418440	0.2104190	0.8391561	3.196038	6.00000	6

table have been obtained following the above procedure.

Now the upper portion of Table II portrays $I_{\mathbf{r}}$ of CHO and PISB at five r_c values introduced before; the respective $I_{\mathbf{p}}$ of two systems are produced in lower segment. There is no literature result available for any of these quantities for comparison. It is interesting to note that, for FHO and CHO in a state having $m = 0$, $I_{\mathbf{r}}$ and $I_{\mathbf{p}}$ are directly related to expectation values of kinetic and potential energy as;

$$I_{\mathbf{r}}(\omega) = 8\langle T\rangle, \quad I_{\mathbf{p}}(\omega) = \frac{64}{\omega^2}\langle v(r)\rangle. \tag{14}$$

But for a PISB, total energy is solely kinetic energy as the potential energy is zero. However, one can evaluate $I_{\mathbf{r}}, I_{\mathbf{p}}$ for PISB and compare the results with CHO. Because, a pair of systems having same $I_{\mathbf{r}}, I_{\mathbf{p}}$ for all states indicate identical physical and chemical environment. Hence, here we have used I to investigate the characteristics of PISB and CHO at $r_c \to 0$.

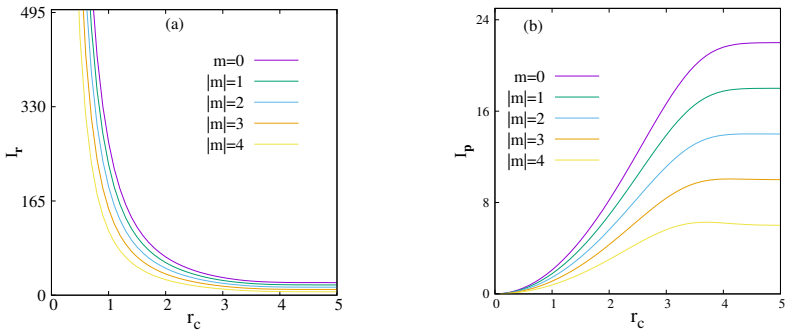


FIG. 1: Variation of $I_{\mathbf{r}}$ and $I_{\mathbf{p}}$ in CHO, with r_c, for all allowed $|m|$ values of $1g$ state, in panels (a) and (b) respectively. See text for details.

The table clearly demonstrates that at $r_c \to 0$, a CHO has comparable $I_{\mathbf{r}}, I_{\mathbf{p}}$ values with that of PISB, thus confirming our presumption that, at $r_c \to 0$, CHO behaves like a PISB. One also notices that, with reduction in r_c, $I_{\mathbf{p}}$ (and also potential energy) approaches *zero*. On the other hand, as r_c grows, the separation between $I_{\mathbf{r}}$ (also $I_{\mathbf{p}}$) values of CHO and PISB tends to extend significantly. Moreover, as expected, at $r_c \to \infty$, CHO reduces to FHO. Elsewhere [8, 9] it has been reported that, a 1D CHO may be treated as a two-mode system; at smaller (approaching zero) and larger (tending infinity) confinement lengths it behaving like a particle in a box and an FHO respectively. Here, also we observe analogous behavior. At $r_c \to 0$ and ∞, CHO leads to PISB and a 3D isotropic FHO respectively. We also note that, larger the value of ω higher will be $\langle v(r) \rangle$; as a consequence CHO is more prone to FHO in such a case. On the contrary, lesser the ω, $\langle v(r) \rangle$ is smaller and CHO, in that occasion, resembles more to a PISB. Therefore at a fixed r_c, by modulating ω values one can investigate properties of all three systems starting from PISB to FHO through CHO.

So far, we have been discussing about the limiting trend of CHO. Now we turn focus on to its behavior at intermediate r_c region. For that, at first, the dependence of $I_{\mathbf{r}}, I_{\mathbf{p}}$ on quantum number n_r is recorded in Table S1 of Supplementary Material (SM). It tabulates these quantities for lowest five n_r (0-4) at six representative r_c. This plainly implies that, at fixed m, l and r_c, both $I_{\mathbf{r}}, I_{\mathbf{p}}$ in CHO get incremented as n_r assumes higher values. Henceforth, the role of n_r on these measures is not discussed any further.

Now, in order to get a better picture of the effect of magnetic quantum number, Table III gives $I_{\mathbf{r}}, I_{\mathbf{p}}$ of CHO for lowest three circular states having $l \neq 0$, i.e., $1p$-$1f$ respectively, for all possible m. Likewise, Fig. 1 displays these for $1g$ state in panels (a) and (b), for all permitted $|m|$ at 6 carefully selected r_c $(0.1, 0.5, 1, 2, 7, \infty)$. Once again, no literature works exist along

these lines; hopefully they would be useful for future referencing. It is to be noted that, the quantities in last column at $r_c = \infty$ are given from Eq. (12) considering $\omega = 1$. For this special ω, Eq. (12) dictates that, $I_{\mathbf{r}} = I_{\mathbf{p}}$ for FHO. One notices that, behavior of $I_{\mathbf{r}}$ and $I_{\mathbf{p}}$ in CHO is always in consonance with FHO; a thorough analysis suggests identical patterns. In general, $I_{\mathbf{r}}$ decays monotonically while $I_{\mathbf{p}}$ progresses with advancement of r_c; this is found to hold good for all $|m|$. This is to be expected, as a growth in r_c facilitates delocalization in r space and localization in p space. At a certain r_c and fixed quantum numbers n_r and m, $I_{\mathbf{r}}$ tends to grow with l; this is consistent to what is observed from Eq. (12) in FHO. Because, in both CHO and FHO, kinetic energy gains with n_r, l. Similarly, at a fixed n_r, l, in both CHO and FHO, $I_{\mathbf{r}}$ lessens as one descends down the table (increment in $|m|$). One striking fact is that, for all these three states considered, both CHO and FHO portray similar pattern with respect to m. Next, I_t for $1s$-$1f$ states of CHO are offered in Table S2 of SM. It seems to show a propensity towards $I_{\mathbf{r}}$ in the behavioral pattern. In all instances, the lower and upper bounds governed by Eq. (11) is satisfied. For an arbitrary state distinguished by quantum numbers n_r, l, variation in $I_{\mathbf{r}}, I_{\mathbf{p}}$ with r_c in a CHO preserves same qualitative orderings for various m (general nature of the plots remain unchanged) as depicted in these figures. This has been verified in multiple occasions, which are not reported here to save space. As usual, in all cases, they all eventually approach their respective CHO-limit at some sufficiently large r_c, which varies from state to state.

Now to understand the effect of l on $I_{\mathbf{r}}, I_{\mathbf{p}}$, we offer Table IV, where these are listed for $l = 1 - 9$ states having $|m| = 1$ and n_r corresponding to 1, at same six chosen r_c's of previous table. As earlier, here too, no reference work is known to us. The last column again has same significance as Table III. In accordance with Eq. (12), here also for $2l$ states, $I_{\mathbf{r}} = I_{\mathbf{p}}$ in FHO. Dependence of $I_{\mathbf{r}}, I_{\mathbf{p}}$ of CHO on l parallels our observation in FHO. At a given n_r, m and r_c, they both get incremented with rise of l in CHO and FHO. This may occur presumably because that, as l progresses, the density gets increasingly concentrated. Therefore, at fixed n_r, m, a state with higher l experiences greater oscillation. Thus all our foregoing discussion leads to a general fact that, the qualitative variations of $I_{\mathbf{r}}$ with all three quantum numbers remain quite similar to that of $I_{\mathbf{p}}$ in a CHO; also the trends in CHO and FHO are analogous. It may be appropriate to mention a parallel work [30] along this line for free and confined H atom inside an impenetrable spherical enclosure. One finds several significant deviations in the variation pattern between two systems there. Here we

TABLE IV: $I_{\mathbf{r}}, I_{\mathbf{p}}$ for $2p$-$2m$ ($|m| = 1$) states in CHO, at six selected r_c. See text for details.

l	$r_c = 0.1$	$r_c = 0.5$	$r_c = 1$	$r_c = 2$	$r_c = 7$	$r_c = \infty$
			$I_{\mathbf{r}}$			
1	19544.75146	781.7758499	195.3902144	48.61008407	14.000000000	14
2	28201.56829	1128.0488516	281.9599554	70.272141773	18.000000000	18
3	37976.00550	1519.027385	379.70865634	94.73419843	22.0000000000	22
4	48838.86407	1953.5428786	488.3419262	121.91517166	26.0000000000	26
5	60766.49285	2430.649110	607.62258270	151.75456390	30.0000000001	30
6	73739.4732	2949.5692932	737.3562778	184.204055587	34.0000000743	34
7	87741.58879	3509.6547640	877.38084537	219.22364350	38.00000037	38
8	102759.07974	4110.3551463	1027.5587357	256.77944910	42.0000017797	42
9	118780.106607	4751.196872	1187.77161130	296.84230573	46.0000074341	46
			$I_{\mathbf{p}}$			
1	0.01221	0.3054	1.222	4.917	14.000	14
2	0.0133333	0.333337	1.33356	5.34750	18.00000	18
3	0.014439157	0.36097833	1.4438781	5.7743588	21.999997	22
4	0.0154743767	0.38685628	1.54723822	6.1782594	26.0000000	26
5	0.016426161	0.4106495	1.6423270	6.55303527	30.000000	30
6	0.017296672	0.4324115849	1.7293332625	6.898114452	34.00000	34
7	0.0180927445	0.4523131126	1.808922468	7.21517631	38.00000	38
8	0.0188222240	0.470550071	1.88186836	7.50667165	41.9999991	42
9	0.019492648	0.487310795	1.94891804	7.775182	45.99998	46

mention two of the most interesting facts, which are in direct contrast with a CHO, e.g., $I_{\mathbf{r}}$ remains invariant with respect to changes in l, whereas under confinement, it reduces with l (at fixed n, m). Besides, for a given state having fixed n, m, $I_{\mathbf{p}}$ progresses when the atom is compressed, whereas declines in a free H atom.

Before concluding, a few words may be devoted to the influence of ω on $I_{\mathbf{r}}, I_{\mathbf{p}}$. In order to probe this, Fig. 2 depicts plots of $I_{\mathbf{r}}$ and $I_{\mathbf{p}}$ against r_c, for 5 selected ω^2 $(1, 2, 4, 8, 32)$, in bottom ((a), (b)) and top ((c), (d)) panels. These are given for $1p$ state; left and right panels characterize $|m| = 0$ and 1 respectively. Evidently at a given r_c, $I_{\mathbf{r}}$ grows and $I_{\mathbf{p}}$ decays with increment in ω. At a fixed ω, dependence of these measures on n_r, l, m is similar to that in FHO. As ω goes up, there is more localization, hence compactness in single-particle density enhances with oscillation strength.

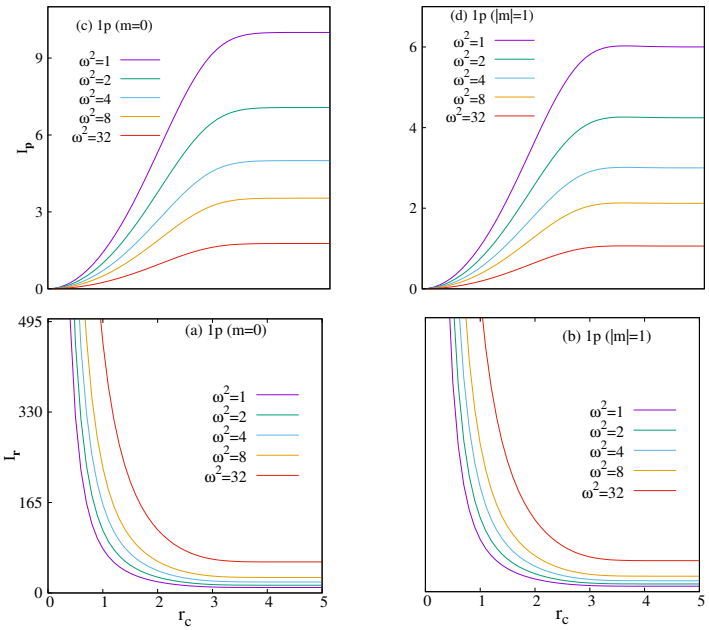


FIG. 2: Plots of $I_{\mathbf{r}}$ and $I_{\mathbf{p}}$ in bottom ((a), (b)) and top ((c),(d)) panels in CHO with r_c, of $1p$ state at five selected $\omega^2(1, 2, 4, 8, 32)$. Left, right columns correspond to $|m| = 0$, 1 respectively.

IV. FUTURE AND OUTLOOK

Benchmark values of $I_{\mathbf{r}}, I_{\mathbf{p}}, I_t$ are offered in a CHO, for both $l = 0$ and $l \neq 0$ states with special emphasis on the latter. Representative results are provided for $1s$-$1g$ as well as $2s$-$2m$ states. A CHO may be considered as a two-mode system; at $r_c \to 0$ it behaves as a PISB and at $r_c \to \infty$ it reduces to an FHO. Effect of m on these measures has been analyzed in detail. To the best of our knowledge, such an examination in CHO is pursued here as a first case. With progress in r_c, $I_{\mathbf{r}}$ falls and $I_{\mathbf{p}}$ rises. These are compared and contrasted with FHO results; in all aspects they show analogous trends. Further, their changes with respect to ω is also registered. This work suggests that, I may be employed to predict various properties of physically important systems. Therefore, further inspection of I in other free and confinement situations may be worthwhile and could be taken up in future.

V. ACKNOWLEDGEMENT

Financial support from DST SERB, New Delhi, India (sanction order: EMR/2014/000838) is gratefully acknowledged. NM thanks DST SERB, New Delhi,

India, for a National-post-doctoral fellowship (sanction order: PDF/2016/000014/CS).

---

[1] A. Michels, J. de Boer and A. Bijl, Physica **4**, 981 (1937).

[2] J. R. Sabin, E. Brändas and S. A. Cruz (Eds.), *The Theory of Confined Quantum Systems*, Parts I and II, Advances in Quantum Chemistry, Vols. 57 and 58 (Academic Press, 2009).

[3] K. D. Sen (Ed.), *Statistical Complexity: Applications in Electronic Structure* (Springer, 2012).

[4] K. D. Sen (Ed.), *Electronic Structure of Quantum Confined Atoms and Molecules* (Springer, Switzerland, 2014).

[5] N. Aquino and R. A. Rojas, Eur. J. Phys. **37**, 015401 (2016).

[6] R. M. Yu, L. R. Zan, L. G. Jiao and Y. K. Ho, Few-Body Syst. **58**, 152 (2017).

[7] H. Pang, W-S. Dai and M. Xie, J. Phys. A **44**, 365001 (2011).

[8] V. G. Gueorguiev, A. R. P. Rau and J. P. Draayer, Am. J. Phys. **74**, 394 (2006).

[9] H. Laguna and R. P. Sagar, Ann. Phys. (Berlin) **526**, 555 (2014).

[10] V. C. Aguilera-Navarro, E. Ley Koo and A. H. Zimerman, J. Phys. A **13**, 3585 (1980).

[11] H. Taşeli, Int. J. Quant. Chem. **46**, 319 (1993).

[12] G. Campoy, N. Aquino and V. D. Granados, J. Phys. A **35**, 4903 (2002).

[13] H. E. Montgomery Jr. , G. Campoy and N. Aquino, Phys. Scr. **81**, 045010 (2010).

[14] A. K. Roy, Mod. Phys. Lett. A **30**, 1550176 (2015).

[15] G. Barton, A. J. Bray and J. McKane, Am. J. Phys. **58**, 751 (1990).

[16] D. H. Berman, Am. J. Phys. **59**, 937 (1991).

[17] A. C. Tanner, Am. J. Phys. **59**, 333 (1991).

[18] N. Aquino, E. Castaño, G. Campoy and V. Granados, Eur. J. Phys. **22**, 645 (2001).

[19] L. Stevanović, AIP Conf. Proc. **1203**, 1188 (2010).

[20] A. Ghosal, N. Mukherjee and A. K. Roy, Ann. Phys. (Berlin) **528**, 796 (2016).

[21] F. M. Fernández and E. A. Castro, Phys. Rev. A **24**, 2883 (1981).

[22] V. C. Aguilera-Navarro, J. F. Gomes, A. H. Zimerman and E. Ley-Koo, J. Phys. A **16**, 2943 (1983).

[23] N. Aquino, J. Phys. A **30**, 2403 (1997).

[24] K. D. Sen and A. K. Roy, Phys. Lett. A **357**, 112 (2006).

[25] H. E. Montgomery Jr., N. A. Aquino and K. D. Sen, Int. J. Quant. Chem. **107**, 798 (2007).

[26] Lj Stevanović and K. D. Sen, J. Phys. B **41**, 225002 (2008).

[27] A. K. Roy, Mod. Phys. Lett. A **29**, 1450104 (2014).

[28] B. R. Frieden, *Science from Fisher Information* (Cambridge University Press, London, 2004).

[29] N. Mukherjee and A. K. Roy, Int. J. Quant. Chem. (in press)

[30] N. Mukherjee, S. Majumdar and A. K. Roy, Chem. Phys. Lett. **691**, 449 (2018).

[31] S. Majumdar, N. Mukherjee and A. K. Roy, Chem. Phys. Lett. **687**, 322 (2017).

[32] D. Chakraborty and P. W. Ayers, in *Statistical Complexity: Applications in Electronic Structure*, K. D. Sen (Ed.), pp. 35 (Springer, 2012).

[33] I. V. Toranzo, P. Sánchez-Moreno, R. O. Esquivel and J. S. Dehesa, Chem. Phys. Lett. **614**, 1 (2014).

[34] Á. Nagy and K. D. Sen, Phys. Lett. A **360**, 291 (2006).

[35] K. D. Sen, C. P. Panos, K. Ch. Chatzisavvas and Ch. C. Moustakidis, Phys. Lett. A **364**, 286 (2007).

[36] Á. Nagy, Chem. Phys. Lett. **425**, 154 (2006).

[37] R. González-Férez and J. S. Dehesa, Eur. Phys. J. D **32**, 39 (2005).

[38] E. Romera, P. Sánchez-Moreno and J. S. Dehesa, Chem. Phys. Lett. **414**, 468 (2005).

[39] J. S. Dehesa, A. Martínez-Finkelshtein and V. N. Sorokin, Mol. Phys. **104**, 613 (2006).

[40] W. A. Yahya, K. J. Oyewumi and K. D. Sen, Int. J. Quant. Chem. **115**, 1543 (2015).

[41] B. J. Falaye, K. J. Oyewumi, S. M. Ikhdair and M. Hamzavi, Phys. Scr. **89**, 115204 (2014).

[42] J. O. A. Idiodi and C. A. Onate, Commun. Theor. Phys. **66**, 269 (2016).

[43] C. A. Onate and J. O. A. Idiodi, Commun. Theor. Phys. **66**, 275 (2016).

[44] M. S. Abdelmonem, A. Abdel-Hady and I. Nasser, Mol. Phys. **115**, 1480 (2017).

[45] J. Sañudo and R. López-Ruiz, Phys. Lett. A **372**, 5283 (2008).

[46] A. I. Aptekarev, D. N. Tulyakov, I. V. Toranzo and J. S. Dehesa, Eur. Phys. J. D **89**, 85 (2016).

[47] J. S. Dehesa, I. V. Toranzo and D. Puertas Centeno, Int. J. Quant. Chem. **117**, 48 (2016).

[48] A. K. Roy, J. Phys. G **30**, 269 (2004).

[49] A. K. Roy, A. F. Jalbout and E. I. Proynov, Int. J. Quant. Chem. **108**, 827 (2008).

[50] A. K. Roy, Int. J. Quant. Chem. **113**, 1503 (2013); *ibid.*, **114**, 383 (2014).

[51] A. K. Roy, Int. J. Quant. Chem. **115**, 937 (2015); *ibid.*, **116**, 953 (2016).

[52] S. H. Patil, K. D. Sen, N. A. Watson and H. E. Montgomery Jr., J. Phys. B **40**, 2047 (2007).

[53] C. Cohen-Tannoudji, B. Diu and F. Laloe, *Quantum Mechanics*, Vols. 2 (John Wiley & Sons., 1978).

arXiv:1904.03013v1 [quant-ph] 4 Apr 2019

Supplemental Materials: Fisher information in confined isotropic harmonic oscillator.

TABLE S1: $I_{\mathbf{r}}, I_{\mathbf{p}}$ for lowest five n_r ($l = 0$) values at six different r_c. See text for details.

n_r	$r_c = 0.1$	$r_c = 0.5$	$r_c = 1$	$r_c = 2$	$r_c = 7$	$r_c = \infty$
			$I_{\mathbf{r}}$			
0	3947.84176	157.9137401	39.48285935	10.130828577	6.00000000	6
1	15791.3670	631.654662	157.91245186	39.42241043	14.00000000	14
2	35530.57584	1421.2230213	355.3049651	88.77709457	22.00000000	22
3	63165.46816	2526.6187189	631.6541846	157.88183967	30.00000000	30
4	98696.0440	3947.8417551	986.960106	246.718681361	38.00000000	38
			$I_{\mathbf{p}}$			
0	0.0113069007	0.2825333012	1.1217967676	3.9877029335	6.0000000	6
1	0.01282672989	0.32070687721	1.28512015257	5.25470219890	14.0000000	14
2	0.0131081767	0.3277292039	1.3124046596	5.34276239849	22.00000000	22
3	0.0132066828	0.3301825760	1.3216621568	5.3463257844	30.00000000	30
4	0.0132522770	0.33131731951	1.3258940221	5.3437134181	38.00000000	38

TABLE S2: I_t for $1p$-$1f$ ($n_r = 0$) orbitals at six different r_c. See text for details.

$\|m\|$	$r_c = 0.1$	$r_c = 0.5$	$r_c = 1$	$r_c = 2$	$r_c = 7$	$r_c = \infty$
			$I_t(1p)^a$			
0[†]	121.01515	120.98286	120.491051	113.776614	100.00000000	100
1	57.53752	57.5166	57.1034	55.318	36.0000	36
			$I_t(1d)^b$			
0[†]	233.15973	233.117506	232.518248	223.80357	196.000000000	196
1	138.93098	138.89164	138.3419	130.2598	100.00000	100
2	68.870938	68.8380	68.3884	61.8358	36.00000	36
			$I_t(1f)^c$			
0[†]	380.432960	380.388051	379.716077	369.644758	324.0000000	324
1	255.126029	255.083860	254.452650	244.935911	196.00000	196
2	154.706834	154.669915	154.117184	145.762637	100.00000	100
3	79.1753741	79.1461919	78.7096703	72.1249096	36.00000	36

[†] These also correspond to upper bounds, given in Eq. (10).

[a] Lower bounds Eq. (11), for $1p$ at 6 r_c are: 10.70940, 10.71226, 10.75598, 11.39074, 12.96, 12.96.

[b] Lower bounds Eq. (11), for $1d$ at 6 r_c are: 5.55842, 5.559428, 5.573756, 5.79079, 6.61224, 6.61224.

[c] Lower bounds Eq. (11), for $1f$ at 6 r_c are: 3.40664, 3.40704, 3.41307, 3.506068, 4, 4.